Microstructural, Tribology, and Densification Studies of Spark Plasma Sintered Titanium Matrix Composites Reinforced with Silicon Carbide

Peter Ifeolu Odetola
Tshwane University of Technology
Abimbola Patricia Popoola
Tshwane University of Technology
Emmanuel Ajenifuja (eajenifuja@gmail.com)
Tshwane University of Technology https://orcid.org/0000-0002-8832-8267
Olawale Popoola
Tshwane University of Technology

Research Article

Keywords: TMCs, silicon carbide, spark plasma sintering, microstructure, densification, tribology

Posted Date: March 26th, 2020

DOI: https://doi.org/10.21203/rs.3.rs-19369/v1

Microstructural, Tribology, and Densification Studies of Spark Plasma Sintered Titanium Matrix Composites Reinforced with Silicon Carbide

Peter Ifeolu Odetola[1*], Abimbola P.I. Popoola[1], Emmanuel Ajenifuja[1,2,3], Olawale Popoola[2]

[1]Department of Chemical, Metallurgical and Materials Engineering, Tshwane University of Technology, Pretoria West, Pretoria 0183, South Africa.

[2]Center for Energy and Electric Power, Tshwane University of Technology, Pretoria, South Africa.

[3]Center for Energy Research and Development, Obafemi Awolowo University, Ile-Ife, Nigeria.

Abstract

Spark plasma sintered titanium matrix composites (TMCs) with varying SiC contents were fabricated at 900ºC, 150ºC/min, 30 MPa, and with 5 min of holding time, and were studied for structural, mechanical and tribology performances. The phase identification and microstructure analysis of the sintered specimens were examined using X-ray diffraction and scanning electron microscope equipped with EDS. The results indicate that influence of the varied SiC content dictate the physical properties of the sintered TMCs. The densification study showed that relative density was inversely related, while Vickers hardness value was directly proportional (238.84 Hv at 1 wt. % SiC and 361.81 Hv 6 wt. % SiC). The tribology study showed that both wear rate and coefficient of friction have inverse relationship while wear resistance has a direct trend with the composite reinforcement. Sample TiNiAl – 6 wt. % SiC, with the optimum composition had the best wear performance under the constant load of 20 N. This wear performance can be attributed to the good interfacial bond formed between the TiNiAl matrix and the SiC reinforcement in the developed composites contributed from the synergetic processing conditions of the SPS process.

Keywords: TMCs, silicon carbide, spark plasma sintering, microstructure, densification, tribology.

Introduction

Novel materials with tailored properties evolve daily through composite technology. This makes the engineering use of materials more plausible for critical applications. Good temperature strength and improved tribological characteristics are the primary performance criteria for the selection of composites for most engineering applications, particularly in aerospace and automotive sectors. The mechanical properties and microstructural characteristics of such materials are key considerations for their suitability and compatibility. Material properties are often impaired under critical conditions of elevated temperatures, stringent chemical species, and incessant mechanical vibrations, thereby compromising their integrity by fatigue, creep, stress, or cracking to sustain application.

Primarily, titanium is considered an ideal aerospace material due to its high strength-to-weight ratio, lightweight, corrosion-resistant, and substantial thermal stability **[1-4].** In the aerospace industry, titanium plays a leading role as a base material with the flexibility to combine with a significant number of metals (especially nickel and aluminium) and ceramics (oxides, carbides, or organic base) to form their alloys and composites **[5-8].** This flexibility enables powder metallurgist to fabricate new titanium matrix-based materials with enhanced properties suitable for sustaining the system prone to mechanical vibration conditions, chemical species, and stringent temperature profiles.

Titanium matrix composites (TMCs) can be fabricated from monolithic titanium or its alloy, which serves as the base matrix for the infusion of second phase particles (reinforcements). **Odetola et al. [9]** established that the property profiles of TMCs can be easily upgraded through the right reinforcement match. Generally, the strength of composites is determined by the fabrication process, grain size (microns or nanoscales), composition (measuring the distribution of the weight percentage of the matrix phase compared to the reinforcement phase), and microstructure **[10,11].** These dictate physical and mechanical properties of composite materials **[11,13].**

In TMCs fabrication, the use of discontinuous reinforcement as second-phase particles has gained the most recognition as low-cost sintering aids with the ability to enhance material efficiency. A good discontinuous reinforcement is such that is thermodynamically stable at sintering temperature, and insoluble in titanium or its alloy matrix. In terms of reinforcing materials, silicon carbide (SiC) has been identified as a promising sintering aid for enhancing strength-to-weight ratio, wear capacity, high temperature strength, and corrosion performance of TMCs **[14-17].**

In the production of particulate-reinforced composite, homogeneous distribution of the second-phase particles in the matrix is very vital for superior performance. Besides this, the reinforcing phase is also susceptible to agglomeration, which may deteriorate mechanical properties. However, the difficulty of obtaining a clean matrix-reinforcement interface free from undesired secondary phases can be easily rectified with processing conditions that can minimize or eliminate common challenges such as porosity, segregation, agglomeration, de-bonding, grain pullout and atomic misfit. Spark plasma sintering is an exceptional powder metallurgy technique capable of bridging deficiency gap in the solid sintering of powders at elevated temperatures due to its remarkable processing conditions such as faster heating rates and lower temperature requirements at short holding times **[18].** Therefore, difficult-to-sinter powder materials with very high or low melting points or excessive reactivity can easily be sintered with ease **[4,13, 19-21].**

In this work, spark plasma sintering was used to fabricate silicon reinforced titanium matrix composites (TiNiAl-SiC). Densification studies, as well as microstructural and mechanical characterization, were used to evaluate and determine property profiles in a variety of reinforcement compositions (1,3, and 6 wt. %). Densification studies are used to evaluate the quality of SPSed composites in terms of porosity level, as well as accompanied properties.

2 Materials and Method

2.1 Materials

The powder combination chosen for fabrication are titanium, nickel, and aluminium (matrix supplied by TLS Technik, particle size of range 45-90 μm, and percentage purity of 99.9%) and silicon carbide (reinforcement supplied by F.J. Brodman & Co., L.L.C., approximate particle size of ~ 22 μm, and 99.9% pure). The microstructural templates of their initial characterization are presented in Fig. 1. The design of the work permits the varied composition of the SiC (1, 3, and 6 wt.%) in the matrix at fixed SPS process conditions of 900^{o}C, 150^{o}C/min, 30 MPa, and 5 min holding time as shown in Table 1.

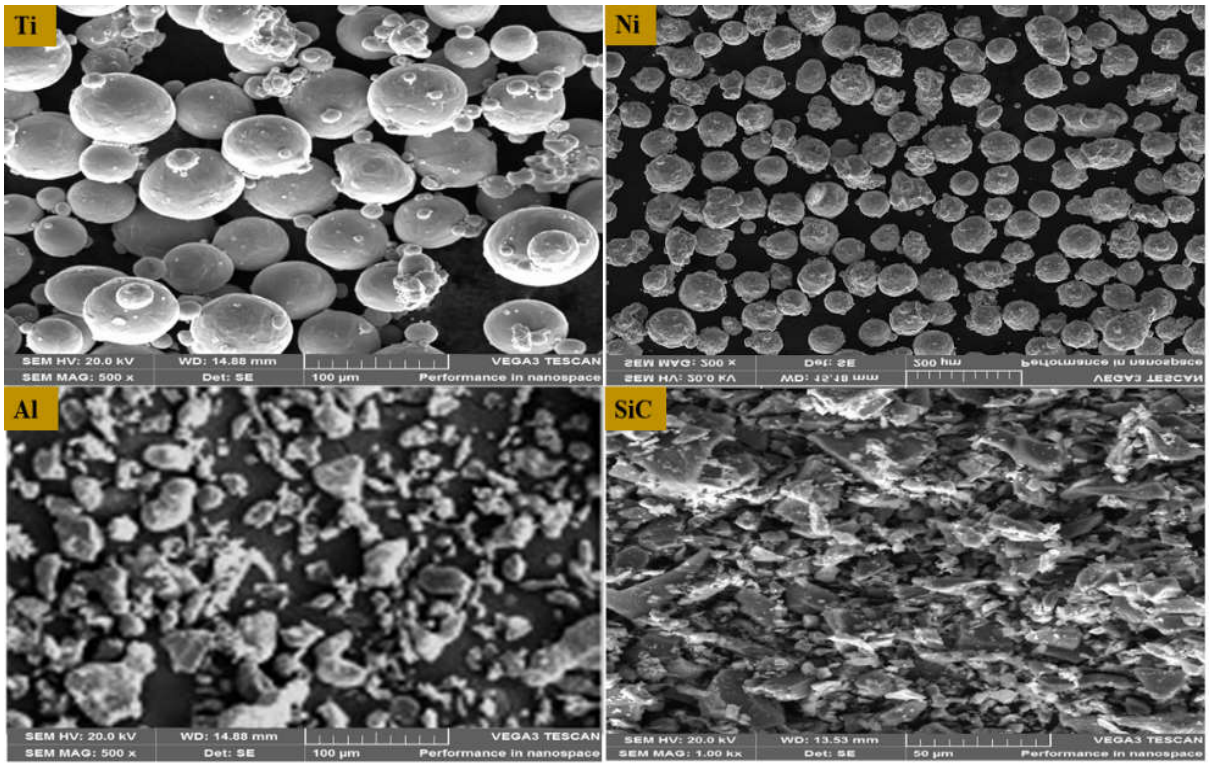

Fig. 1: SEM initial powder characterization of Ti, Ni, Al, and SiC

Table 1: Composition details of composite powders

Composite Samples	**Compositions, wt.%**
Control - TiNiAl	*87%* Ti + *10%* Ni + *3%* Al
TiNiAl-*1 wt.%* SiC	*86%* Ti + *10%* Ni + *3%* Al + *1%* SiC
TiNiAl-*3 wt.%* SiC	*84%* Ti + *10%* Ni + *3%* Al + *3%* SiC
TiNiAl-*6 wt.%* SiC	*81%* Ti + *10%* Ni + *3%* Al + *6%* SiC

2.2 Method

2.2.1 Powder preparation

The design of the titanium-based alloy matrix composites was done according to the compositions presented in Table 1. The successive powder batch was thoroughly mixed in a plastic container placed inside a Tubular Shaker Mixer (T2F) operated at a constant rotational speed of 72 rpm for duration of 12 h to attain homogenization.

2.2.2 Composite fabrication

The homogenized powder mixture was charged into Ø30 mm graphite die of the SPS HPD5, FCT Systeme GmbH at sintering conditions of 900 °C, 150 °C/min, 40 MPa and holding time of 5 min. In addition to the control specimen, three different batches of TMCs were fabricated as shown in Table 1. For easy removal of sintered specimen and lowering of temperature gradient across the specimen, graphite sheets were used to demarcate the enclosed powders from direct contact with the die and also from the upper and lower punches as recommended by **Shongwe et al. [22].** At completion of the sintering, the sintered specimens were sand blasted to get rid of graphite contaminations. Prior to any further characterization process, the relative densities of the sintered specimens were measured using Archimedes principle. The theoretical or bulk density of the specimens was calculated using the rule of mixtures based on the densities of raw powders according to equation 1 for control sample and specimens sintered at 1%, 3%, and 6% SiC contents respectively (see Table 1).

$$\boldsymbol{Bulk_{\rho}} = \left(\frac{\boldsymbol{Ti_{wt.\ \%}}}{\boldsymbol{Ti_{\rho}}} + \frac{\boldsymbol{Ni_{wt.\ \%}}}{\boldsymbol{Ni_{\rho}}} + \frac{\boldsymbol{Al_{wt.\ \%}}}{\boldsymbol{Al_{\rho}}} + \frac{\boldsymbol{SiC_{wt.\ \%}}}{\boldsymbol{SiC_{\rho}}}\right)^{-1} \quad ----------(\mathbf{1})$$

Where $\boldsymbol{\rho}$ represents density in $\boldsymbol{g/cm^3}$ and the composition of the participating powders in $\boldsymbol{wt.\%}$ Densification is calculated from the ratio of the relative (experimental) density of each specimen to the corresponding theoretical or bulk density using the principle of rule of mixtures as shown in equation 2. The relationship of densification to porosity is shown in equation 3.

$$\boldsymbol{Densification} = \left(\frac{\boldsymbol{R.D_{\rho}}}{\boldsymbol{T.D_{\rho}}} \times \mathbf{100\%}\right) \quad ----------(\mathbf{2})$$

Where $\boldsymbol{R.D_{\rho}}$ represents relative density in $\boldsymbol{g/cm^3}$ and $\boldsymbol{T.D_{\rho}}$ represents theoretical density of bulk in $\boldsymbol{g/cm^3}$.

$$\boldsymbol{Porosity} = \mathbf{100\%} - \boldsymbol{Densification} \quad ----------(\mathbf{3})$$

2.2.3 Characterization of SPSed specimens

2.2.3.1 Microstructural characterization

Firstly, the specimens were sectioned, properly ground, and polished to reveal smooth mirror-like surface. This is followed by dipping into Nital reagent (100 ml ethanol in 1-10 ml HNO_3) for 10-20 s prior to microstructural examination. The microstructures and the elemental compositions of

the composites were examined with TESCAN scanning electron microscope equipped with an EDS. Also, the microstructures were also viewed under optical microscopy for further in-depth studies.

2.2.3.2 Mechanical characterization

The hardness values were evaluated on a Future-tech 700 microhardness testing machine using the Vickers hardness scale. The specimens were subjected to a 100 gf load with a dwell time of 10 s to evaluate the hardness. An average of seven different hardness indentations was computed for the hardness measure of each sintered specimen.

Table 2: Densification and Hardness of specimens

Specimens	T.D (g/cm^3)	R.D (g/cm^3)	Porosity (%)	Hardness (Hv)
Control – TiNiAl	4.64	99.14	0.86	230.02
TiNiAl-1 wt.% SiC	4.62	98.92	1.08	238.84
TiNiAl-3 wt.% SiC	4.58	98.4	1.60	330.57
TiNiAl-6 wt.% SiC	4.52	97.57	2.43	361.81

2.2.3.3 Densification study

Relative density is an index that illustrates densification progress of the as-sintered powder compacts as well as influences the mechanical performance of sintered specimen such as hardness. The densification study was carried out by comparing the theoretical density of each specimen with their respective relative density using rule of mixtures. Spark plasma sintering has emerged as an efficient sintering technique to consolidate the powders to achieve density almost equal to theoretical density. Densification behavior is expected to be a function of linear shrinkage which in turn depends on the sintering temperature, pressure, time and current intensity.

2.2.3.4 Tribological study

The tribological characteristics of the control and composites specimens were studied using Universal Tribometer s/n RTEC 2441, USA. The wear test was conducted using samples prepared in form of discs Ø10mm and length of 10 mm under load of 20 N for 1000 s and at a speed of 5 Hz. The specimens were weighed initially against hard steel alloy of 350 mm.

Table 3: Densification and Hardness of specimens

Specimen	Wear Rate	Wear Resistance	COF
TiNiAl- *0 wt.%* SiC	0.114	8.772	0.382
TiNiAl-*1 wt.%* SiC	0.078	12.821	0.377
TiNiAl-*1 wt.%* SiC	0.07	14.286	0.372
TiNiAl-*1 wt.%* SiC	0.063	15.873	0.358

3 Results and Discussion

3.1 Microstructure

Representative SEM micrographs and EDS analysis of composites at sintering conditions of 900ºC, 150ºC/min, 30 MPa, and 5 min holding time are presented in Fig. 2 (a) & (b), 3 (a) & (b), and 4 (a) & (b) respectively. The microstructures of the developed TiNiAl – SiC were studied at the minimum, intermediate, and maximum content of the second phase particle (1 wt. % SiC, 3 wt. % SiC, and 6 wt. % SiC) respectively. Physical examination of the entire microstructures in view of their representative EDS mappings established the black flecks as SiC, the dominant greyish areas as TiNiAl matrix zone with rich titanium being the bulk in composition, and the white spherical zones as nickel rich. Some of the SiC particulate was observed to diffuse into the matrix grain forming intermetallics such as Ti_3SiC_2 picked by the XRD spectra for all the specimens. Fig. 2 (a) represents microstructure of TiNiAl – 1 wt. % SiC with minimal distribution of the second phase particle into the matrix at the onset of grain boundary formation. Fig. 3 (a) & (b) represents the SEM micrograph and EDS mapping of TiNiAl – 3 wt. % SiC. The SiC flecks were preferentially located at the grain boundaries of the matrix and the EDS spectrum showed an increase in the SiC content over the microstructural variation. This may be responsible for hardness improvement with increase in content of SiC shown in Table 2. The highest content of SiC in the TiNiAl matrix is represented by Fig. 4 (a), which showed well developed grain boundaries with interlock SiC particulates. The EDS spectra in Fig. 4 (b) also confirmed the maximum abundance of the second-phase particles. This may be responsible for the highest hardness value recorded through strain hardening at the crowded interface between the matrix and the reinforcement phase. Intermetallic like $AlNi_6Si_3$, Ti_3SiC_2, TiNiSi present in this microstructure further support the reason for the enhanced hardness at this optimum addition.

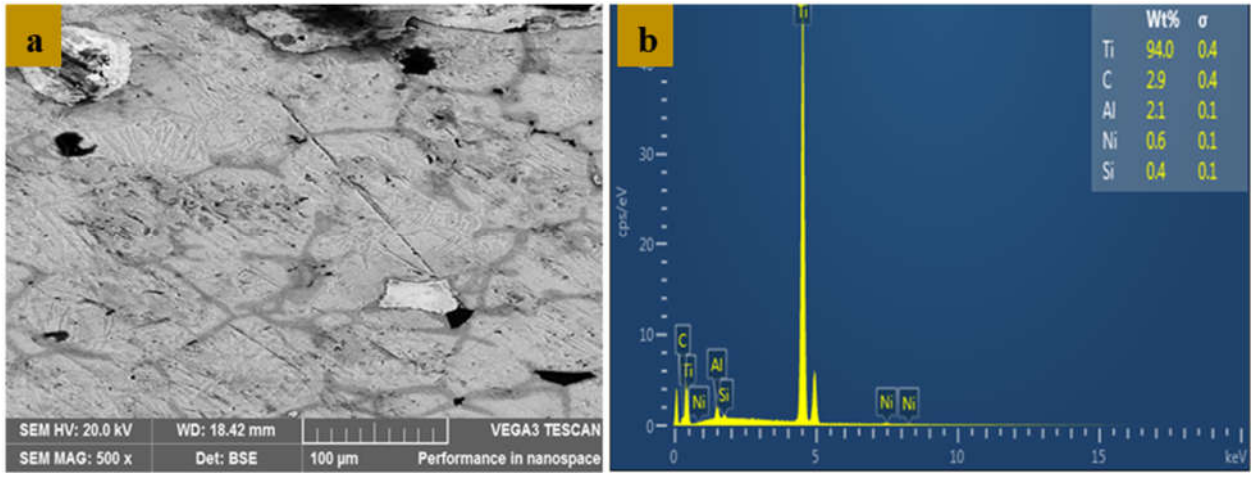

Fig. 2: (a) microstructure and (b) EDS mapping of TiNiAl-1wt.% SiC composite fabricated at 900°C.

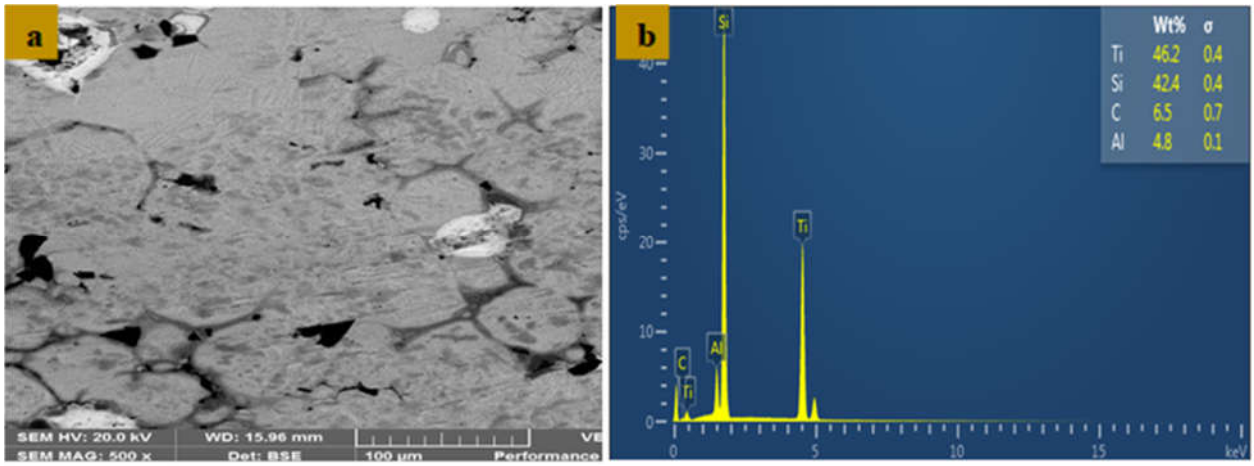

Fig. 3: (a) microstructure and (b) EDS mapping of TiNiAl-3wt.% SiC composite fabricated at 900°C.

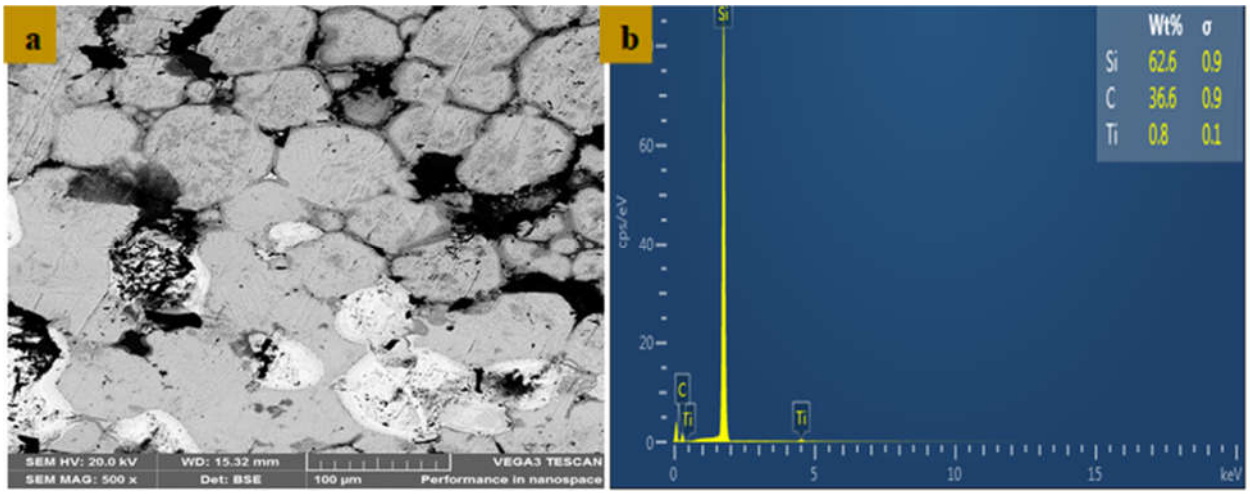

Fig. 4: (a) microstructure and (b) EDS mapping of TiNiAl-6wt.% SiC composite fabricated at 900°C.

Fig. 5 (a-c) are the OPM micrographs of the sintered specimens at 900°C at different weight percentage of SiC powder reinforcement. The control sample is a pure TiNiAl matrix alloy. Fig. 5 (a) representing the minimum addition of SiC showed few black flecks sprouted in the alloy matrix. With subsequent increase in composition of SiC, the growth spread and interlocked mostly at the grain boundaries as shown in Fig. 5 (b). Also, in Fig. 5 (c), there was less pronouncement of the black flecks and numerous needle-like growth, which was as a result of active intermetallic compounds that have been formed. These intermetallic compounds are hard materials formed from the matrix and second phase particle. They gradually build up at the grain boundaries, thereby preventing dislocation movement and causing stain hardness.

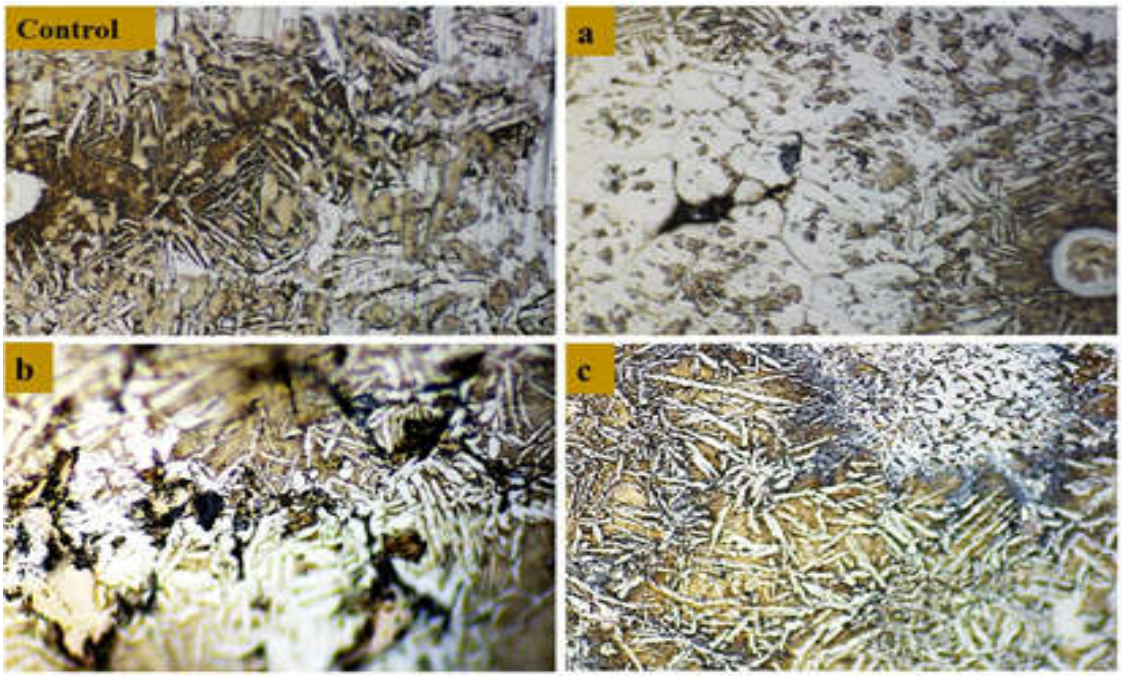

Fig. 5: OPM micrographs of control and TiNiAl-SiC at (a) 1 wt. % (b) 3 wt. %, and (c) 6 wt. %

3.2 Phase (XRD) Analysis

The XRD results for the developed TiNiAl –SiC composites are shown in Fig. 6. The spectra indicate microstructural variations represented by the dominant phases at various peak, most of which are intermetallic compounds with compositions such as Ti_3SiC_2, TiNiSi, and $AlNi_6Si_3$. These intermetallic compounds were not present in the control specimen. In the TiNiAl – 1 wt. % SiC spectrum, the phases are more of alloys formed from the elemental interaction of the matrix such as Ti_2 (peak phase), Ti_2Ni_2, and AlNi while the Ti_3SiC_2 formed justified the minute 1 wt. % SiC

in the composites. As the SiC content increases, a marked difference was observed in the spectra trends showing additional ternary alloy (TiNiAl) and intermetallic compounds at different phases in the specimens.

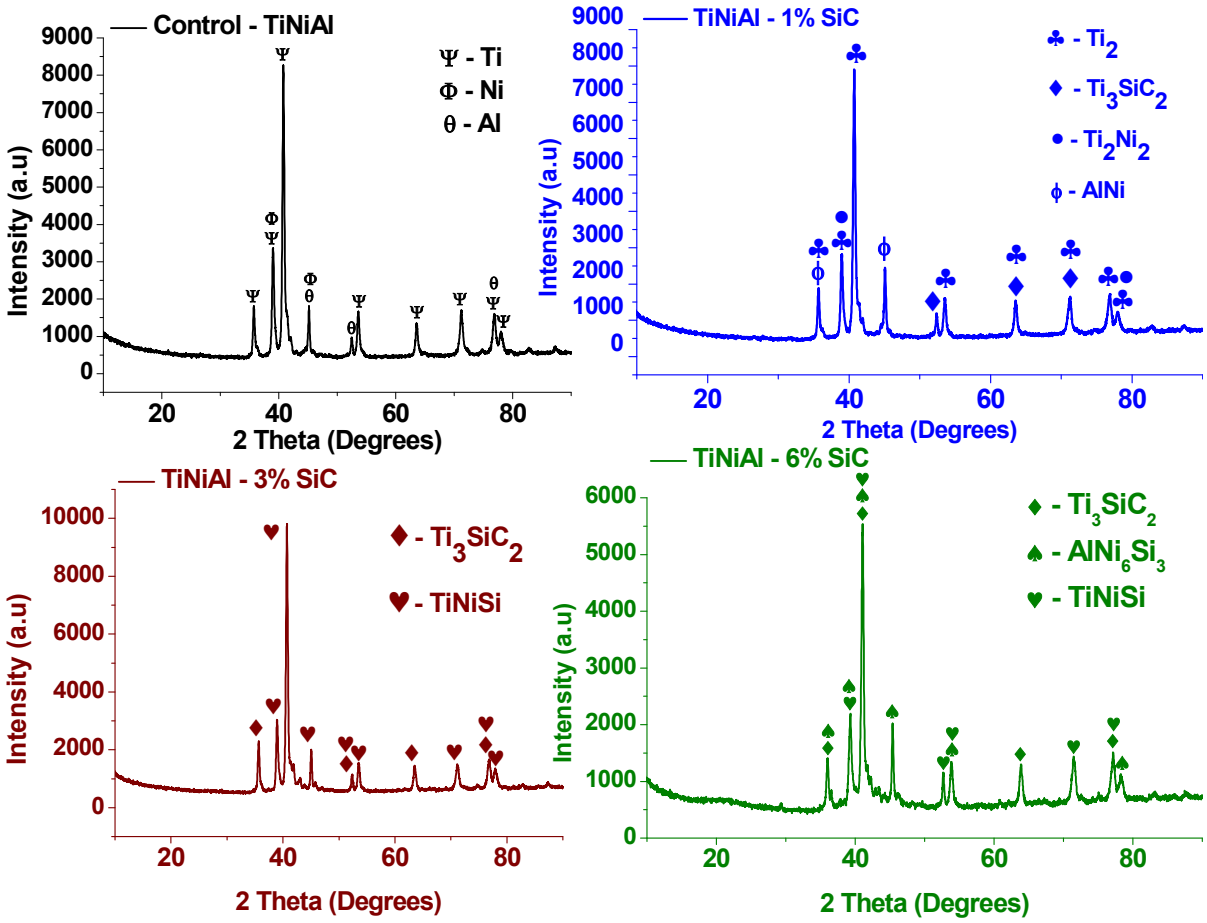

Fig. 6: XRD Spectrum of TiNiAl -SiC composites with different wt.%

The confirmed presence of these intermetallics are responsible for the enhanced hardness profiles of the sintered specimens with increase in the wt. % composition SiC. At sintering temperature of 900ºC, these intermetallics were synergetically formed from the matrix elements (Ti, Ni, Al) and SiC. It is noteworthy that these intermetallic compounds have excellent match of properties viable for tailored applications that require high temperature strength, good corrosion resistance, and electrical integrity. Aside from the control sample, Ti_3SiC_2 intermetallic was present in XRD spetra of all the sintered composite speimens. Primarily, Ti_3SiC_2 is a hard carbide with dual properties of metal and ceramic, which makes it an exceptional material with better combination of thermal and mechanical property than monolithic titanium **[23-28].** Furthermore, it has a superior thermal

shock resistance, higher temperature oxidation resistance, superior fracture toughness and better damage resilience compared to titanium.

3.3 Relative density and hardness

At a constant sintering temperature of 900ºC , relative density was inversely related while hardness value was directly proportional. Fig. 7 shows the variation of relative density and hardness with addition of SiC as a function of wt. % composition. It is obvious that the relative density of the sintered specimen decreased from 98.92% to 97.57% when the SiC content increased from 1% to 6%. This can be explained on the basis of residual pores generated within the matrix since higher activation energy is required for volume diffusion compared to grain boundary diffusion. The sintering was more of volume control than thermodynamically controlled and increase in SiC content at the constant temperature only permits active volume diffusion of grains. On the other hand, hardness enhancement may be attributed to homogeneous dispersion of particles, as well as increasing reinforcement particle content, which eventually lockup with the matrix at the grain boundary **[29, 30].** The lowest, medium, and highest hardness values are 238.84 Hv, 330.57 Hv, 361.81 Hv respectively. Therefore, there was tangible improvement in hardness of about 66% between minimum and optimum reinforcement.

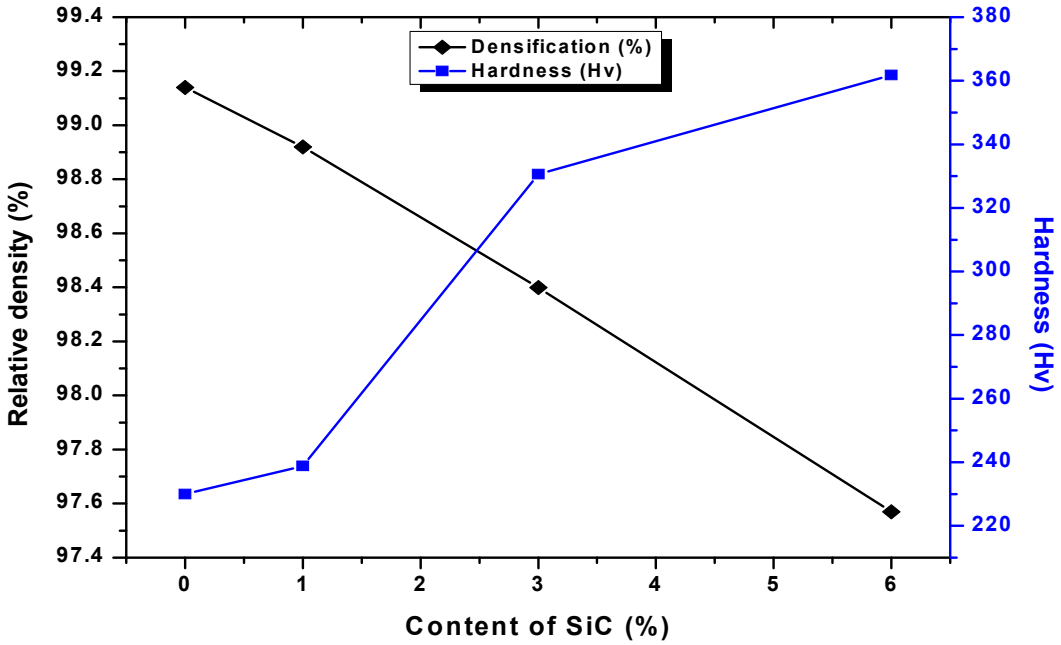

Fig. 7: Relative density and hardness of TiNiAl -SiC composites at different SiC content

3.4 Wear study

3.4.1 Wear behavior

Fig. 8 shows the observed variation of wear parameters at 20 N load for 1000 s and at a speed of 5 Hz. The wear rate, the wear resistance and the coefficient of friction were evaluated with changing SiC content in the TMCs. It was observed that both wear rate and coefficient of friction have inverse relationship while wear resistance has a direct trend with the composite reinforcement, which introduced hard resisting particles into the matrix. The downward trend observed in both wear rate and the coefficient of friction from minimum to optimum addition of SiC can be attributed to the fact that during sliding, hard phases formed were removed from the matrix and the debris got crammed and difficult to displaced further. Therefore, increasing SiC content in the composite resulted into increasing the distribution of the hard SiC phase in the matrix, which tends to reduce the wear loss and thereby improving the wear resistance significantly. From the EDS and XRD carried out shown in Figs. 2 and 6 respectively, the hard phases are intermetallic carbides formed between the matrix and the reinforcement. It is established that TiNiAl – 6 wt. % SiC, which has the optimum composition has the best wear performance under the constant load of 20 N. This outstanding wear performance can be attributed to the good interfacial bond formed between the TiNiAl matrix and the SiC reinforcement in the developed composites contributed from the synergetic processing conditions of the SPS process. In conclusion, the resistance power of the TiNiAl –SiC composites are in the control of composition of the reinforcement, which make them more feasible for tribological applications.

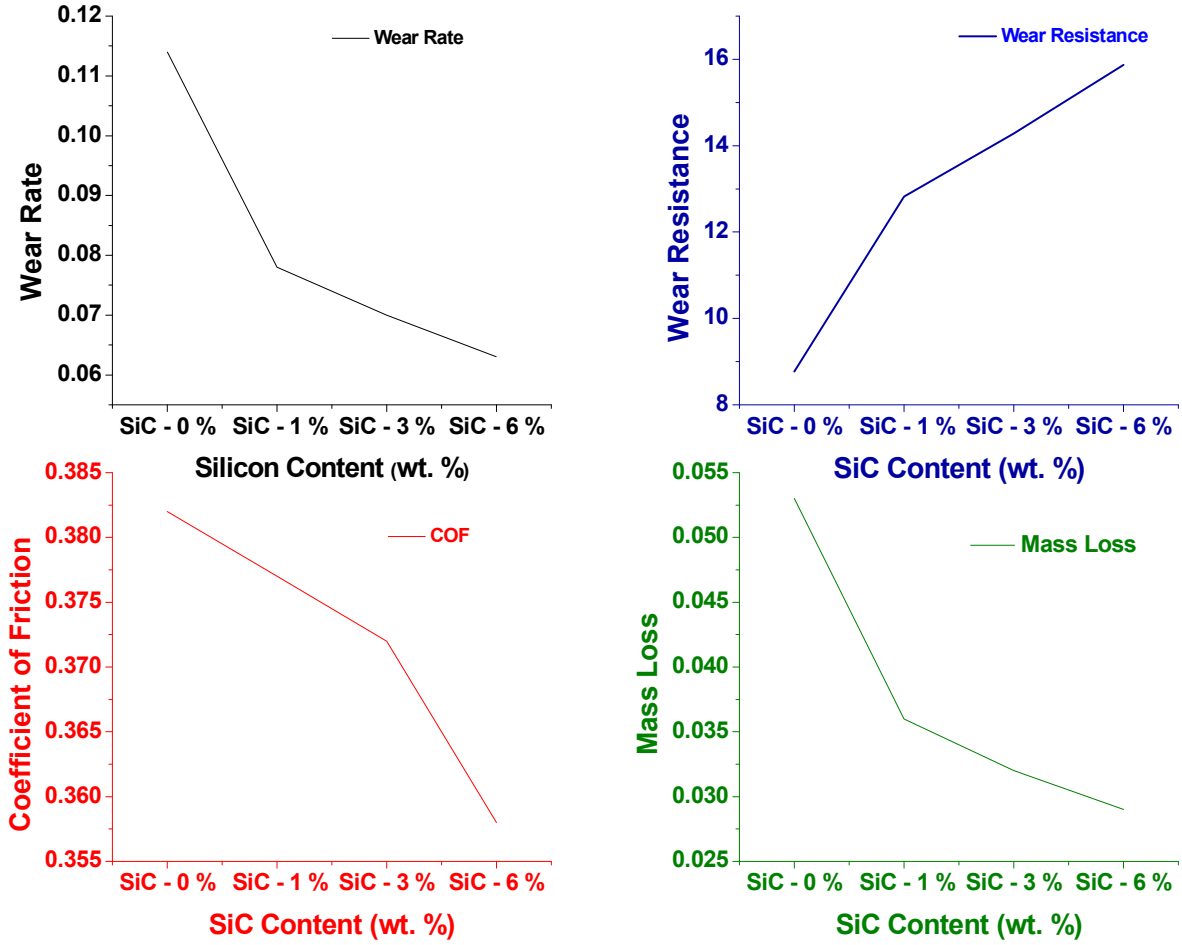

Fiag. 8: Influence of SiC content on tribological preoperties of TiNiAl – SiC composites

Conclusion

In the developed titanium matrix composites (TMCs), the influence of the varied SiC content dictates the densification, microhardness, and tribological performance with the following deduced conclusions

1. Relative density was inversely related to the SiC content (98.92% at 1 wt. % SiC and 97.57% at 6 wt. % SiC). This can be explained on the basis of residual pores generated within the matrix since higher activation energy is required for volume diffusion than for grain boundary diffusion. The sintering being carried out at the same temperature of 900ºC was more of volume control than thermodynamically controlled. Increase in SiC content at this constant temperature only permits active volume diffusion of grains.
2. Vickers hardness value was directly proportional to SiC content (238.84 Hv at 1 wt. % SiC and 361.81 Hv 6 wt. % SiC). The hardness enhancement may be attributed to homogeneous

dispersion of particles, as well as increasing reinforcement particle content, which eventually lockup with the matrix at the grain boundaries.

3. Wear rate and coefficient of friction have inverse relationship while wear resistance has a direct trend with the composite reinforcement, which introduced hard resisting particles into the TiNiAl matrix. Therefore, TiNiAl – 6 wt. % SiC, which has the optimum composition had the best wear performance under the constant load of 20 N. This shows that increasing the SiC content is beneficial to reducing wear of the developed titanium matrix composites.
4. Titanium matrix composites have been successfully fabricated with outstanding property profiles, which are attributed to the good interfacial bond formed between the TiNiAl matrix and the SiC reinforcement in the developed composites contributed from the synergetic processing conditions of the SPS process.

Acknowledgement

The authors express their gratitude to Tshwane University of Technology, Pretoria, South Africa., for the financial and logistic supports provided to the success of this work. National Research Foundation (NRF) is also acknowledged.

Data Availability

The raw/processed data required to reproduce these findings cannot be shared at this time as the data also forms part of an ongoing study.

References

[1] Peters M, Kumpfert J, Ward CH, Leyens C. Titanium alloys for aerospace applications. Advanced engineering materials. 2003 Jun 26;5(6):419-27.

[2] Campbell FC. Chapter 4—Titanium. Manufacturing Technology for Aerospace Structural Materials; Elsevier Science: Oxford, UK. 2006:119–174.

[3] Campbell FC. Chapter 9—Metal matrix composites. Manufacturing Technology for Aerospace Structural Materials; Elsevier Science: Oxford, UK. 2006:419-57.

[4] Zadra M, Girardini L. High-performance, low-cost titanium metal matrix composites. Materials Science and Engineering: A. 2014 Jul 1; 608:155-63.

[5] Duncan RM, Hanson BH. The selection and use of titanium. Oxford University Press for the Design Council, the British Standards Institution and the Council of Engineering Institutions; 1980.

[6] Leyens C, Peters M, editors. Titanium and titanium alloys: fundamentals and applications. John Wiley & Sons; 2003 Sep 19.

[7] Banerjee D, Williams JC. Perspectives on titanium science and technology. Acta Materialia. 2013 Feb 1;61(3):844-79.

[8] Rosso M. Ceramic and metal matrix composites: Routes and properties. Journal of materials processing technology. 2006 Jun 1;175(1-3):364-75.

[9] Odetola PI, Ajenifuja E, Popoola AP, Popoola O. Effects of silicon carbide contents on microstructure and mechanical properties of spark plasma–sintered titanium-based metal matrix. The International Journal of Advanced Manufacturing Technology. 2019:1-0

[10] Das T, Munroe PR, Bandyopadhyay S. The effect of Al 2 O 3 particulates on the precipitation behaviour of 6061 aluminium-matrix composites. Journal of materials science. 1996 Oct 1;31(20):5351-61.

[11] Emami SM, Salahi E, Zakeri M, Tayebifard SA. Effect of composition on spark plasma sintering of ZrB2–SiC–ZrC nanocomposite synthesized by MASPSyn. Ceramics International. 2017 Jan 1;43(1):111-5.

[12] Gofrey TM, Goodwin PS, Ward-Close CM. Titanium particulate metal matrix composites–Reinforcement, production methods, and mechanical properties. Advanced Engineering Materials. 2000 Mar;2(3):85-91.

[13] Tjong SC, Mai YW. Processing-structure-property aspects of particulate-and whisker-reinforced titanium matrix composites. Composites Science and Technology. 2008 Mar 1;68(3-4):583-601.

[14] Harris GL, editor. Properties of silicon carbide. Iet; 1995.

[15] Pierson HO. Handbook of refractory carbides and nitrides: properties, characteristics, processing and applications. William Andrew; 1996 Dec 31.

[16] Mampuru KM, Ajenifuja E, Popoola O. Effect of silicon carbide addition on the microstructure, hardness and densification properties of spark plasma sintered Ni-Zn-Al alloy. Journal of King Saud University-Science. 2019 Jan 19.

[17] Odetola PI, Popoola AP, Ajenifuja E, Popoola O. Effects of temperature on the microstructure and physico-mechanical properties of TiNiAl-SiC composite by spark plasma sintering technique. Materials Research Express. 2019 May 15;6(8):085802.

[18] Guillon O, Gonzalez-Julian J, Dargatz B, Kessel T, Schierning G, Räthel J, Herrmann M. Field-assisted sintering technology/spark plasma sintering: mechanisms, materials, and technology developments. Advanced Engineering Materials. 2014 Jul;16(7):830-49.

[19] Bhat BR, Subramanyam J, Prasad VB. Preparation of Ti-TiB-TiC & Ti-TiB composites by in-situ reaction hot pressing. Materials Science and Engineering: A. 2002 Feb 28;325(1-2):126-30.

[20] Ni DR, Geng L, Zhang J, Zheng ZZ. Fabrication and tensile properties of in situ TiBw and TiCp hybrid-reinforced titanium matrix composites based on Ti–B4C–C. Materials Science and Engineering: A. 2008 Apr 15;478(1-2):291-6.

[21] Li SF, Sun B, Kondoh K, Mimoto T, Imai H. Influence of carbon reinforcements on the mechanical properties of Ti composites via powder metallurgy and hot extrusion. In Materials Science Forum 2013 (Vol. 750, pp. 40-43). Trans Tech Publications.

[22] Shongwe MB, Diouf S, Durowoju MO, Olubambi PA. Effect of sintering temperature on the microstructure and mechanical properties of Fe–30% Ni alloys produced by spark plasma sintering. Journal of Alloys and Compounds. 2015 Nov 15, 649:824-32.

[23] Barsoum MW, El-Raghy T. Synthesis and characterization of a remarkable ceramic. Ti3SiC2. 1996 Jul;79(7):1953-6.

[24] Barsoum MW. The MN+ 1AXN phases: A new class of solids: Thermodynamically stable nanolaminates. Progress in solid state chemistry. 2000 Jan 1;28(1-4):201-81.

[25] Ho-Duc LH. Synthesis and characterization of the properties of Ti3SiC2/SiC and Ti3SiC2/TiC composites; 2002.

[26] Mogilevsky P, Mah TI, Parthasarathy TA, Cooke CM. Toughening of SiC with Ti3SiC2 particles. Journal of the American Ceramic Society. 2006, 89(2):633-7.

[27] Liu WY, Zhang JB, Jin YM, Hu TT, Chen TT, Xiao XP, Yan LM. Microstructure and properties of Ti3SiC2/Al–Si composites synthesized by spark plasma sintering. Materials Research Express. 2017 Nov 24;4(11):116521.

[28] Chen Y, Shi X, Zhai W, Deng X, Yan Z, Liu X, Lu G, Zhou H. Tribological performance of Ti3SiC2 enhanced Ni3Al matrix composites. Materials Research Express. 2018, 5(6):066528.

[29] Li RT, Dong ZL, Khor KA. Al–Cr–Fe quasicrystals as novel reinforcements in Ti based composites consolidated using high pressure spark plasma sintering. Materials & Design. 2016, 102:255-63.

[30] Steinman AE, Corthay S, Firestein KL, Kvashnin DG, Kovalskii AM, Matveev AT, Sorokin PB, Golberg DV, Shtansky DV. Al-based composites reinforced with AlB2, AlN and BN phases: experimental and theoretical studies. Materials & Design. 2018 Mar 5; 141:88-98.